Carbohydrate Polymers 88 (2012) 676–683

Contents lists available at SciVerse ScienceDirect

Carbohydrate Polymers

journal homepage: www.elsevier.com/locate/carbpol

Comparison of physicochemical properties of starches from seed and rhizome of lotus

Jianmin Man[a,b], Jinwen Cai[a,b], Canhui Cai[a,b], Bin Xu[c], Huyin Huai[b], Cunxu Wei[a,b,*]

[a] Key Laboratories of Crop Genetics and Physiology of the Jiangsu Province and Plant Functional Genomics of the Ministry of Education, Yangzhou University, Yangzhou 225009, PR China
[b] College of Bioscience and Biotechnology, Yangzhou University, Yangzhou 225009, PR China
[c] Testing Center, Yangzhou University, Yangzhou 225009, PR China

ARTICLE INFO

Article history:
Received 21 November 2011
Received in revised form
23 December 2011
Accepted 5 January 2012
Available online 13 January 2012

Keywords:
Lotus
Seed
Rhizome
Starch
Physicochemical property

ABSTRACT

Lotus seed and rhizome starches have been used as functional foods in east Asia for thousands of years. In this paper, starches were isolated from lotus seed and rhizome, and their physicochemical properties were compared. Seed starches were small oval granules, rhizome starches had small oval granules and large elongated granules. Seed starches showed significantly higher amylose content and gelatinization temperature and lower swelling power than rhizome starches. Seed starches exhibited an A-type X-ray diffraction pattern with higher crystalline degree, while rhizome starches showed a C-type pattern which changed from C- to A-type with gradually increasing crystalline degree during acid hydrolysis. The degree of order in starch external region was higher in rhizome than in seed. The external region structure of rhizome starches became more ordered during acid hydrolysis. Rhizome starches had higher rate of acid hydrolysis and lower rate of porcine pancreatic α-amylase hydrolysis than seed starches.

1. Introduction

Lotus (*Nelumbo nucifera* Gaertn.), an aquatic perennial from family Nelumbonaceae, is an important economic plant which is widely cultivated in China, India, Japan and Australia (Wang & Zhang, 2004). Besides its popularity as an ornamental flower, the rhizome of lotus is used as a popular vegetable and can be eaten in roasted, pickles, dried slices and fried forms, which exhibits multiple nutritional properties (Shad, Nawaz, Hussain, & Yousuf, 2011). Lotus seed, which is rich in protein, amino acids, unsaturated fatty acids and minerals, and without heavy metal contamination, is widely used as food in China (Bhat & Sridhar, 2008; Rai, Wahile, Mukherjee, Saha, & Mukherjee, 2006). Lotus is also used as a folk medicine mainly in China, Japan, and India. Its seed is used in folk remedies as a diuretic, cooling agent, antiemetic and as an antidote in the treatment of tissue inflammation and cancer (Liu et al., 2004). The lotus rhizome is used with other herbs to treat fever, sunstroke, diarrhoea, dysentery, dizziness and stomach problems (Lee, Choi, Noh, & Suh, 2005).

Starches from different botanical sources have diverse physicochemical and functional properties. There is rich source of starch in lotus seed and rhizome (Xu & Shoemaker, 1986). Lotus starches are commercially available in China and consumed as breakfast, fast food, traditional confectionery and food additives, especially suitable for callant and senior. The production is rising year by year because of the market need (Zhong, Chen, & We, 2007). Some physicochemical properties of lotus rhizome starches have been reported (Lin et al., 2006; Suzuki et al., 1992; Zhong et al., 2007), but the properties of seed starches are seldom reported.

In this study, starches were isolated from lotus seed and rhizome. Their morphologies, sizes, amylose contents, crystal properties, thermal properties, swelling powers, and hydrolysis properties were investigated. The objective of the present research was to compare the physicochemical properties of starches from lotus seed and rhizome.

2. Materials and methods

2.1. Plant material

Freshly harvested rhizomes and dry mature seeds of lotus (*N. nucifera* Gaertn.) were obtained from a local natural food

Abbreviations: AAG, *Aspergillus niger* amyloglucosidase; ATR-FTIR, attenuated total reflectance-Fourier transform infrared; DSC, differential scanning calorimetry; PPA, porcine pancreatic α-amylase; XRD, X-ray powder diffraction.

* Corresponding author at: College of Bioscience and Biotechnology, Yangzhou University, Yangzhou 225009, PR China. Tel.: +86 514 87997217.
E-mail addresses: cxwei@yzu.edu.cn, yzuwcx@yahoo.com.cn (C. Wei).

0144-8617/$ – see front matter © 2012 Elsevier Ltd. All rights reserved.
doi:10.1016/j.carbpol.2012.01.016

market (Yangzhou City, China). The hard seed coat was removed with the help of a sharp and clean stainless steel knife and the edible cotyledon portion obtained was used to isolate seed starches.

2.2. Isolation of native starches

Native starch granules were isolated following a method described by Wei, Qin, Zhu, et al. (2010) with a slight modification. Briefly, lotus rhizomes were peeled, sliced in small pieces. The dry seed cotyledons were steeped in double-distilled water at 4 °C for 16 h. The rhizome pieces and softened cotyledons were homogenized with ice-cold water in a home blender. The homogenate was squeezed through four layers of cheesecloth by hand. The fibrous residue was homogenized and squeezed twice more with ice-cold water to facilitate the release of starch granules from the fibers. The combined extract was filtered with 100-, 200-, and 300-mesh sieves and centrifuged at 3000 × *g* for 10 min. The yellow gel-like layer on top of the packed white starch granule pellet was carefully scraped off and discarded. The process of centrifugation separation was repeated several times until no dirty material existed. The precipitated starch was further washed with anhydrous ethanol, dried at 40 °C, ground into powders, and passed through a 100-mesh sieve.

2.3. Morphology observation of starches

A starch suspension (1%, w/v) was prepared with 50% glycerol. A small drop of starch suspension was placed on the microscope slide and covered with a coverslip. The starch granule shape and Maltese cross were viewed under the Olympus BX53 polarized light microscope equipped with a CCD camera.

2.4. Particle size analysis of starches

The sizes of starch granules from seed and rhizome were analyzed. Images of starch granules were analyzed using JEDA-801D morphological image analysis system (Jiangsu JEDA Science-Technology Development Co., Ltd, Nanjing, China). More than 2000 starch granules were analyzed per sample. Rhizome starch granules were classified into oval and elongated starch granules according to the ratio of the long/short axis length. Rhizome oval, elongated and total starch granules and seed starch granules were grouped according to the long axis length, and the number of starch granules in each group was counted. Plotting the relative number of starch granules against the long axis length produced a starch granule size–distribution curve.

2.5. Amylose content determination of starches

Amylose content was determined using the iodine adsorption method of Konik-Rose et al. (2007) with some modifications. About 10 mg of starch (accurate to 0.1 mg) was put into a 10 ml screw-capped tube, then dissolved in 5 ml of urea dimethyl sulfoxide (UDMSO) solution. The dissolution was carried out by incubating at 95 °C for 1 h with intermittent vortexing. An 1 ml aliquot of the starch–UDMSO solution was treated with 1 ml of iodine solution (0.2% I_2 and 2% KI, w/v) and made up to 50 ml volume with water. The blend was immediately mixed and placed in the darkness for 20 min. Apparent amylose content was evaluated from absorbance at 620 nm. The recorded values were converted to percent of amylose by reference to a standard curve prepared with amylose from potato and amylopectin from corn (Sigma–Aldrich).

2.6. Crystal structure analysis of starches

Crystal structure of starch was analyzed on an X-ray powder diffraction (XRD) (D8, Bruker, Germany). The XRD analysis and relative crystalline degree (%) of the starches were carried out following the method described by Wei, Qin, Zhou, et al. (2010). Before measurements, all the specimens were stored in a desiccator where a saturated solution of NaCl maintained a constant humidity atmosphere (relative humidity = 75%) for 1 week.

2.7. Ordered structure analysis of starch external region

Ordered structure of starch external region was analyzed on a Varian 7000 Fourier transform infrared (FTIR) spectrometer with a DTGS detector equipped with an attenuated total reflectance (ATR) single reflectance cell containing a germanium crystal (45° incidence-angle) (PIKE Technologies, USA) as previously described by Wei, Xu, et al. (2010). The assumed line shape was Lorentzian with a half-width of 19 cm^{-1} and a resolution enhancement factor of 1.9.

2.8. Thermal property determination of starches

Thermal property of starch was measured using a differential scanning calorimetry (DSC) (200-F3, NETZSCH, Germany) as described previously by Wei et al. (2011). Starch (~5 mg, dry starch basis) was precisely weighed and mixed with 3 times (by weight) deionized-distilled water (~15 μl). The mixture was sealed in an aluminum pan overnight at 4 °C. After equilibrating for 1 h at room temperature, the starch sample was then heated from 25 to 110 °C at a rate of 10 °C/min.

2.9. Swelling power determination of starches

Swelling power of starch was determined by heating starch–water slurries in a water bath at temperatures ranging from 45 to 95 °C in 5 °C intervals according to the procedures of Wei et al. (2011).

2.10. Hydrolysis property determination of starches

Starches were hydrolyzed by porcine pancreatic α-amylase (PPA) (Sigma–Aldrich), *Aspergillus niger* amyloglucosidase (AAG) (Sigma–Aldrich) and HCl. The hydrolysis rates of starches by PPA and AAG were analyzed using the method of Li, Vasanthan, Hoover, and Rossnagel (2004) with some modifications. For PPA hydrolysis, isolated native starch (10 mg) was suspended in 2 ml of enzyme solution (0.1 M phosphate sodium buffer, pH 6.9, 25 mM NaCl, 5 mM $CaCl_2$, 0.02% NaN_3, 50 U PPA). For AAG hydrolysis, starch (10 mg) was suspended in 2 ml of enzyme solution (0.05 M acetate buffer, pH 4.5, 5 U AAG). The hydrolyses of PPA and AMG were conducted in a constant temperature shaking water bath with continuous shaking (100 rpm) at 37 and 55 °C, respectively. The hydrolysis rate of starches by HCl was analyzed using the method of Wei, Xu, et al. (2010) with minor modification. 20 mg starch was suspended in 2 ml of 2.2 M HCl and hydrolysis was conducted in a constant temperature shaking water bath with continuous shaking (100 rpm) at 35 °C. After hydrolysis, starch slurries were quickly centrifuged (3000 × *g*) at 4 °C for 10 min. The supernatant was used for measurement of the solubilized carbohydrates to quantify the degree of hydrolysis by the anthrone-H_2SO_4 method (Wei, Xu, et al., 2010).

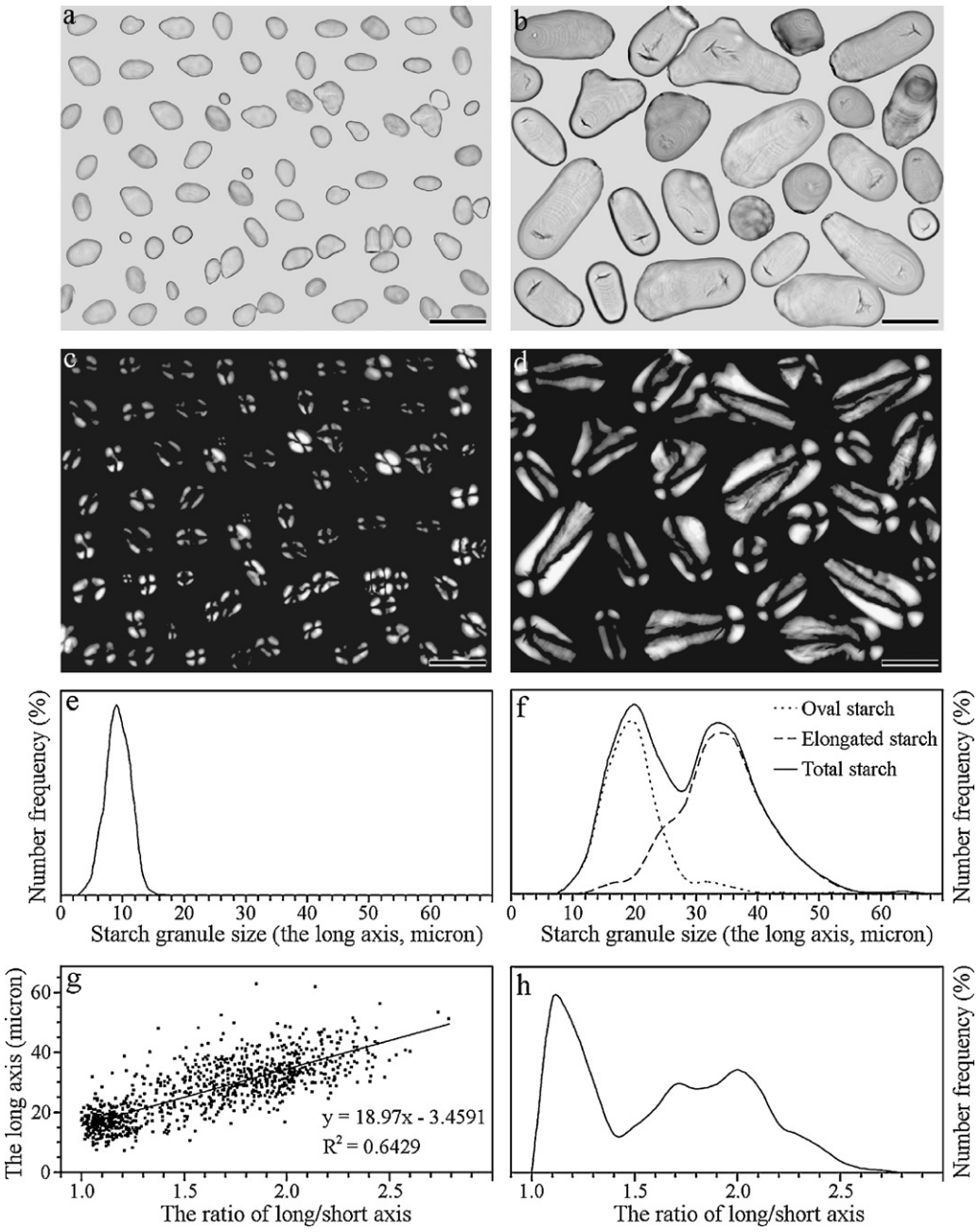

Fig. 1. Morphology and size–distribution of lotus starches. (a, c, e) Seed starches; (b, d, f–h) rhizome starches; (a, b) light microscope graphs; (c, d) polarized light microscope graphs; (e–h) size–distribution curve of starch granules. Scale bar = 20 μm.

3. Results and discussion

3.1. Morphology and size distribution of starches

Photomicrographs taken from light microscope and polarized light microscope of lotus seed and rhizome starches are presented in Fig. 1. Seed starches showed small oval-shaped granules (Fig. 1a). Compared with seed starches, rhizome starches were significantly bigger, and had different morphology. Rhizome starch granules were mostly elongated in shape with relative larger size, some starch granules were oval in shape with relative smaller size. Some irregular starch granules were also observed in rhizome starches (Fig. 1b). The hilum, the original growing point, is usually less structurally organized than the rest of the granule. The hilum is clearly visible in large starch granule owing to its different refractive index under the light microscope (Pérez, Baldwin, & Gallant, 2009). For lotus seed and rhizome oval starch granules, the hilum was at the center of the granule (Fig. 1a and b). For rhizome elongated starch granule, the hilum was not central, but was located near one end of the granule (Fig. 1b). Large hydrated starch granules show as concentric growth rings, which are layers of alternating high and low refractive index (Pérez et al., 2009). The centrical stripes of the growth rings could be observed in lotus rhizome large elongated and irregular starch granules (Fig. 1b). The oval and elongated starch granules in lotus rhizome have also been reported in Lin et al. (2006)'s result. It was noteworthy that there were some fissures and cracks around the hilum of lotus rhizome elongated starch granule (Fig. 1b), which was also reported by Lin et al. (2006) and Zhong et al. (2007). Starches are semicrystalline granules. As a consequence of their crystallinity, most starch granules show a Maltese cross when

viewed with the polarized light microscope. The hilum is the center of the Maltese cross (Pérez et al., 2009). For lotus seed starch, the typical Maltese cross was in the central position (Fig. 1c). For lotus rhizome starch, oval starch granule had a clear central Maltese cross, but the Maltese cross in elongated starch was at one end of granule (Fig. 1d). The difference in granule morphology may be attributed to the biological origin, biochemistry of the amyloplast and physiology of the plant (Sandhu, Singh, & Kaur, 2004).

Starch granule sizes are usually measured by electrozone, image analysis, or laser light-scattering analysis methods. Harrigan (1997) found that using image analysis to determine starch granule size could yield accurate and reproducible data. Therefore, in this study, image analysis was used to determine starch granule size distribution. Fig. 1e and f shows plots of number percent of particles over a range of the long axis length. Lotus seed starches showed unimodal size distribution at 3–16 μm. Rhizome starches exhibited a bimodal size distribution, the first peak was at 8–28 μm, and the second peak was at 28–56 μm. Fig. 1g shows the plot of the long axis length over the ratio of long/short axis length. This plot indicated that the long axis length had a positive correlation with the ratio of long/short axis length. According to the ratio of long/short axis length, rhizome total starch granules might be divided into two populations. Starch granule with the ratio of long/short axis length below 1.4 was oval in shape, while starch granules with the ratio of long/short axis length above 1.4 was elongated in shape. Fig. 1h shows the plot of number percent of particle over the ratio of long/short axis length, which was also showed that the ratio of 1.4 was an index to divide rhizome starches into two parts: oval and elongated starches. In rhizome starches, the oval starches accounted for about 40% of the total granule number, and the elongated starches accounted for about 60%. The plots of number percent of oval and elongated starches in total starches over the long axis length are shown in Fig. 1f, which was agreement with the result of total starch size distribution. The statistical analysis of particle size is shown in Table 1. The average particle size (the long axis length) was 9.73, 26.63, 17.86 and 34.42 μm for lotus seed starch, rhizome total starch, rhizome oval starch and rhizome elongated starch, respectively (Table 1). The average particle size of lotus rhizome total starch was significantly smaller in this study than that (50.27 μm) determined by laser light-scattering analysis in Zhong et al. (2007)'s study. This difference between their values and ours seemed to stem mainly from the different assay method.

3.2. Amylose content of starches

The amylose content plays an important role in starch internal quality. However, only few studies on amylose content from lotus rhizome have been reported (Lin et al., 2006; Suzuki et al., 1992). The amylose contents of lotus seed and rhizome starches were determined in this study to reveal starch internal quality (Table 2). Seed starches showed significantly higher amylose content than rhizome starches. The amylose content of lotus rhizome starch (23.9%) in this study was higher than that (17.4%) in Suzuki et al. (1992)'s study, and lower than that (30.6%) in Zhong et al. (2007)'s study. The differences between their values and ours seemed to stem mainly from the different assay methods used and partly from differences in variety and/or growth conditions.

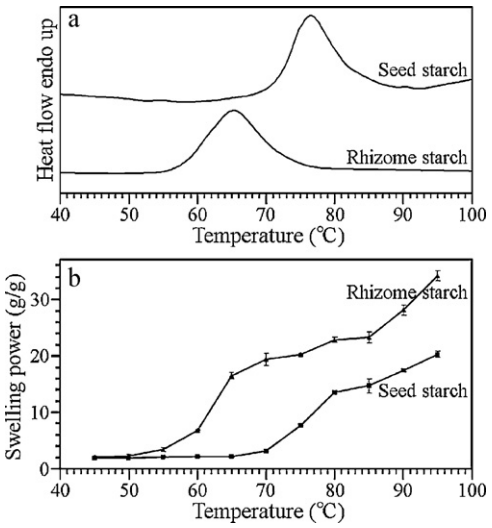

Fig. 2. DSC thermograms (a) and swelling powers (b) of lotus seed and rhizome starches.

3.3. Thermal property of starches

DSC measures and records the amount of heat involved in the starch gelatinization. The gelatinization property of starch is related to a variety of factors including the size, proportion and kind of crystalline organization, and ultrastructure of the starch granules (Lindeboom, Chang, & Tyler, 2004). Fig. 2a presents the gelatinization thermograms of lotus seed and rhizome starches, and their thermal parameters are given in Table 2. The gelatinization temperatures (*To*, *Tp*, and *Tc*) were significantly higher in seed starches than in rhizome starches, while the range temperature (*Tc* – *To*) was significantly lower in seed starches than in rhizome starches. No significant difference was found between the gelatinization enthalpies of seed and rhizome starches.

3.4. Swelling power of starches

According to starch gelatinization temperatures (Table 2), the swelling powers of lotus seed and rhizome starches were investigated from 45 °C to 95 °C in 5 °C intervals (Fig. 2b). Before gelatinization, swelling powers slightly increased with increasing temperature. After gelatinization, swelling power quickly increased. A sharp increase in swelling power of rhizome starch was observed from 55 °C, while that in seed starch was from 70 °C. Seed starch had a much lower swelling power throughout the range of temperatures (70–95 °C) compared with that of rhizome starch.

Swelling power tests are simple analyses that measure the uptake of water during the gelatinization of starch. Amylopectin is considered to contribute to water absorption and swelling and pasting of starch granules, whereas amylose tends to retard these

Table 1
Sizes of lotus seed and rhizome starches.

Length	Seed starch[a]	Rhizome starch		
		Total starch[a]	Oval starch[b]	Elongated starch[c]
Long axis length (μm)	9.73 ± 1.99	26.63 ± 9.76	17.86 ± 5.12	34.42 ± 7.52
Short axis length (μm)	6.69 ± 1.35	16.61 ± 3.85	16.61 ± 3.85	17.33 ± 3.56

[a] Data were means ± standard deviations, $n > 2000$.
[b] The ratio of long/short axis length < 1.4.
[c] The ratio of long/short axis length ≥ 1.4.

Table 2
Thermal properties of lotus seed and rhizome starches.[a]

Starches	Amylose contents (%)	Thermal parameters[b]				
		To (°C)	*Tp* (°C)	*Tc* (°C)	ΔT (°C)	ΔH (J/g)
Seed	38.89 ± 0.68	70.7 ± 0.4	75.8 ± 0.2	82.7 ± 0.3	12.0 ± 0.4	11.1 ± 0.5
Rhizome	23.86 ± 0.28*	57.3 ± 0.3*	64.7 ± 0.1*	72.8 ± 0.4*	15.5 ± 0.5*	10.7 ± 0.4

[a] Data were means ± standard deviations, $n = 3$ for amylose contents and 2 for thermal parameters.
[b] *To*, onset temperature; *Tp*, peak temperature; *Tc*, conclusion temperature; ΔT, gelatinization range ($Tc - To$); ΔH, enthalpy of gelatinization.
* The data of rhizome starch were significantly different ($p < 0.05$) compared with that of seed starch.

processes (Tester & Morrison, 1990). The linear amylose diffuses out of the swollen granules and makes up the continuous phase outside the granules as a restraint to swelling. So, an inverse correlation is found between amylose content and swelling power (Hermansson & Svegmark, 1996). Lotus seed starch had significantly higher amylose content than rhizome starch (Table 2), which might partly explain the lower swelling power of seed starch.

3.5. Crystal property of starches

XRD has been used to reveal the presence and characteristics of crystalline structure of starch granules. According to XRD pattern, there are three types of starch crystalline reported, known as A-, B-, and C-type. A-type crystal starches have strong diffraction peaks at about 15° and 23° 2θ, and an unresolved doublet at around 17° and 18° 2θ. B-type crystal starches give the strongest diffraction peak at around 17° 2θ, a few small peaks at around 15°, 20°, 22°, and 24° 2θ, and a characteristic peak at about 5.6° 2θ. C-type crystal starch is a mixture of both A- and B-type crystalline, and can be further classified to C_A-type (closer to A-type), C-type and C_B-type (closer to B-type) according to the proportion of A-type and B-type polymorphs. The typical C-type crystal starches show strong diffraction peaks at about 17° and 23° 2θ, and a few small peaks at around 5.6° and 15° 2θ. The XRD patterns of C_A- and C_B-type crystal starches show some slight differences from that of typical C-type. C_A-type crystal starches show a shoulder peak at about 18° 2θ and strong peaks at about 15° and 23° 2θ, which are indicative of the A-type pattern. C_B-type crystal starches show two shoulder peaks at about 22° and 24° 2θ and a weak peak at about 15° 2θ, which are indicative of the B-type pattern. The peak at 15° 2θ is strongest in A-type crystalline and weakest in B-type crystalline (Cheetham & Tao, 1998).

The XRD spectra of starches isolated from lotus seed and rhizome are shown in Fig. 3. Seed starches showed a typical A-type XRD pattern, while rhizome starches exhibited a typical C-type pattern (Fig. 3). In general, cereal seed starches give an A-type pattern, tuber and high-amylose cereal starches give a B-type pattern, and legume and *Dioscorea* rhizome starches present a C-type pattern (Cheetham & Tao, 1998; Wang, Yu, Yu, Chen, & Pang, 2007). Both C-type and B-type crystallines have been reported for lotus rhizome starch. For examples, Suzuki et al. (1992) and Zhong et al. (2007) reported that lotus rhizome starches showed a B-type XRD pattern, while Lii and Lee (1993) and Lin et al. (2006) suggested that the lotus rhizome starch had a C-type XRD pattern. These differences suggested that the crystalline structure of lotus starch was easily affected by temperature and some other conditions (Zhong et al., 2007).

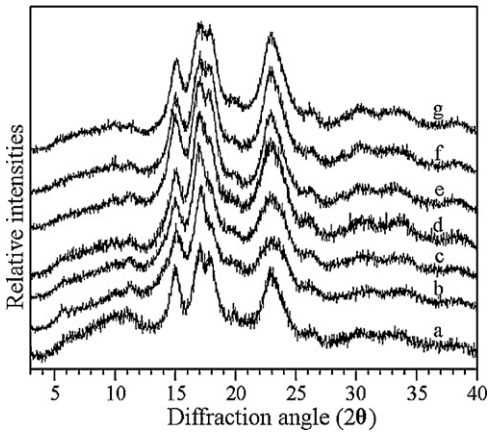

Fig. 3. XRD spectra of Lotus seed and rhizome starches. (a) Native seed starch; (b) native rhizome starch; (c–g) acid-modified rhizome starches for 1 d (c), 2 d (d), 4 d (e), 8 d (f) and 12 d (g).

C-type starch is consisted of A-type and B-type polymorphism within the granule, which is worth further investigating the allomorph distribution. Acid modification does not change the crystalline characteristics of A-type and B-type starches, and is commonly used to investigate the allomorph distribution of C-type starch (Wang et al., 2007). Lotus rhizome starches were hydrolyzed by HCl. The XRD spectra of acid modified starches are shown in Fig. 3. The intensity of the peak at 5.6° 2θ, which was the characteristic of B-type pattern, was found to decrease and disappear with increasing hydrolysis time, and the peak at around 17° 2θ split into two unresolved doublet at around 17° and 18° 2θ, which was the typical A-type characteristic. Sharpening of the peak at 23° 2θ was also observed during acid hydrolysis. The disappearance of the characteristic B-type diffraction peak and the development of typical A-type diffraction peak showed that the crystal type of native lotus rhizome starch changed from typical C-type to A-type pattern, which was not consistent with that of A-type or B-type acid-modified starches which exhibited the same crystalline type as the unmodified starch (Lawal, Adebowale, Ogunsanwo, Barba, & Ilo, 2005; Wang et al., 2007). This result revealed that the B-type polymorphs in the C-type lotus rhizome starch was first degraded or degraded faster than A-type polymorphs in the process of acid hydrolysis. Generally, starch granule was hydrolyzed by HCl from interior to outer region. Therefore, the crystalline changes of acid-modified lotus rhizome starches indicated that the B-polymorphs existed in the interior of C-type starch granules, which was surrounded by the A-type polymorphs at the periphery of starch granule. This crystalline granular structure of lotus rhizome starch was similar to that of C-type starches from pea seed and *Dioscorea* rhizome (Bogracheva, Morris, Ring, & Hedley, 1998; Wang et al., 2007).

The degrees of crystalline of lotus starches calculated from the ratio of diffraction peak area and total diffraction area are given in Table 3. Lotus seed starch showed higher crystalline degree than rhizome starch, though the amylose content in seed starch was higher than that in rhizome starch. Usually, the crystalline degree is negatively correlated with the level of amylose, and A-type starch has significantly higher crystalline degree than B-type or C-type starch at similar amylose content. The higher crystalline degree of lotus seed starch might result from the A-type crystalline. The crystalline degree of acid-modified starches increased with increasing the hydrolysis time. The amorphous region of starch granule was firstly hydrolyzed which resulted in a high content of crystalline

Table 3
Crystalline degree and IR ratio of absorbances for lotus seed and rhizome starches.

Starches	Crystalline degree (%)	IR ratio of absorbances	
		1045/1022 (cm^{-1})	1022/995 (cm^{-1})
Native seed starch	29.0	0.58	1.08
Native rhizome starch	23.3	0.72	0.89
Acid-modified rhizome starch for 1 d	28.0	0.74	0.87
Acid-modified rhizome starch for 2 d	33.5	0.77	0.80
Acid-modified rhizome starch for 4 d	37.5	0.80	0.79
Acid-modified rhizome starch for 8 d	39.9	0.85	0.71
Acid-modified rhizome starch for 12 d	41.7	0.96	0.69

regions. It has been suggested that cleavage of starch chains in the amorphous regions allows extensive reordering of the chain segments to give a more crystalline structure with a sharper X-ray pattern (Wang & Wang, 2001).

3.6. Ordered structure of starch external region

The development of sampling devices like ATR-FTIR combined with procedures for spectrum deconvolution provides opportunities for the study of starch external region structure (Sevenou, Hill, Farhat, & Mitchell, 2002). The deconvoluted ATR-FTIR spectra in the region 1200–900 cm^{-1} of lotus seed and rhizome starches are presented in Fig. 4. The bands at 1045 and 1022 cm^{-1} are linked with order/crystalline and amorphous regions in starch, respectively. The ratio of absorbance 1045/1022 cm^{-1} is used to quantify the degree of order in starch samples. Intensity ratios of 1045/1022 and 1022/995 cm^{-1} are useful as a convenient index of FTIR data in comparisons with other measures of starch conformation (Sevenou et al., 2002). The relative intensities of FTIR bands at 1045, 1022, and 995 cm^{-1} were recorded from the baseline to peak height, and the ratios for 1045/1022 and 1022/995 cm^{-1} were calculated as shown in Table 3.

On the basis of both the spectra and calculated data, native lotus seed and rhizome starches showed significantly different (Fig. 4 and Table 3). Though FTIR is not able to differentiate starch crystal type. The starches with same crystal type always show the similar FTIR spectra, the band at 1022 cm^{-1} is more pronounced in A-type starch than in B-type or C-type starches (Sevenou et al., 2002). Our results showed that the IR ratio of 1045/1022 cm^{-1} was lower in seed starch than in rhizome starch, and the IR ratio of 1022/995 cm^{-1} was higher in seed starch than in rhizome starch. This difference resulted from starch crystal type, and was agreement with the report of Sevenou et al. (2002).

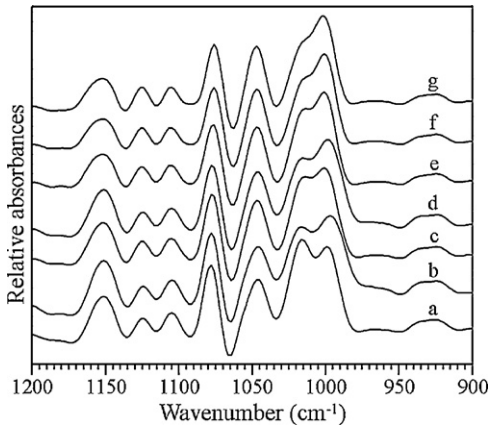

Fig. 4. Deconvoluted ATR-FTIR spectra of lotus seed and rhizome starches. (a) Native seed starch; (b) native rhizome starch; (c–g) acid-modified rhizome starches for 1 d (c), 2 d (d), 4 d (e), 8 d (f) and 12 d (g).

The ATR-FTIR results of rhizome starches showed two remarkable changes during acid hydrolysis (Fig. 4 and Table 3). First, the band at 1022 cm^{-1} was sensitive to acid hydrolysis, whereas the band at 1045 and 995 cm^{-1} was not. Second, the IR ratio of 1045/1022 cm^{-1} increased and that of 1022/995 cm^{-1} decreased with increasing time of acid hydrolysis. This result indicated that the external region structure became more ordered, and the amorphous starch was faster hydrolyzed than crystal starch.

3.7. Hydrolysis property of starches

The hydrolysis degrees of lotus seed and rhizome starches by HCl are presented in Fig. 5a. The hydrolysis degree increased gradually with increasing acid hydrolysis time. Two phases were distinguished in the acid hydrolysis of starch as a function of time. The initial rapid hydrolysis phase was mainly attributed to the hydrolysis of amorphous material from days 0 to 6 for seed starch and 0 to 4 for rhizome starch, and the later slower phase to the hydrolysis of the crystalline region after days 6 for seed starch and 4 for rhizome starch. Several hypotheses have been proposed for the protection of crystalline parts. First, hydrogen ions are unable to penetrate the highly dense packing of double helices within the starch crystallites. Second, a high activation energy is required for

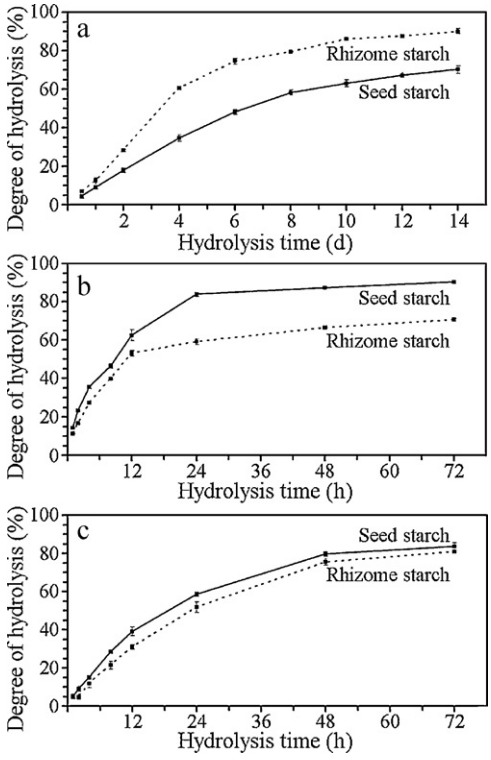

Fig. 5. Hydrolysis of lotus seed and rhizome starches by HCl (a), PPA (b) and AAG (c).

a conformation change in glucose unit from a chair to a half-chair in order to be hydrolyzed (Srichuwong, Isono, Mishima, & Hisamatsu, 2005). The amorphous areas of the starch granules have a looser structure than the crystalline regions which are easier to attack with the hydrogen ions. Native starches have some flaws on the surface of the granules which can provide channels for the infiltration of hydrogen ions. These hydrogen ions primarily get to the amorphous areas and attack them (Wang & Wang, 2001). Susceptibility to acid degradation of the starch granules is found to depend on plant origin. Lotus seed starch had lower rate of acid hydrolysis than rhizome starch. High amylose starch was reported to be less susceptible to acid hydrolysis than normal and waxy starches. It was suggested that the highly compact amorphous regions in high amylose starch granules, resulting from extensive interchain associations of amylose polymers, prevented penetration of acid into the granules (Li, Vasanthan, Rossnagel, & Hoover, 2001). Lotus seed starch had higher amylose content than rhizome starch, which might partly explain why seed starch was slowly hydrolyzed by acid than rhizome starch. Otherwise, rhizome starch granule had marked fissures and cracks around the hilum (Fig. 1), which also facilitated acid hydrolysis.

The time course of PPA hydrolysis of lotus seed and rhizome starches is presented in Fig. 5b. The hydrolysis was biphasic, a relatively rapid rate at the initial stage (0–12 h), followed by a progressively decreased rate thereafter. A biphasic α-amylase hydrolysis trend has also been observed in legume starches with an initial rapid hydrolysis of the amorphous region followed by a decreased hydrolysis (Zhou, Hoover, & Liu, 2004). Lotus rhizome starch had a high resistance to PPA hydrolysis. After 72 h of hydrolysis, the extent of hydrolysis was only about 70.5% for rhizome starch, which was significantly lower than that of seed starch (90.3%) (Fig. 5b). Amylase hydrolysis involves an enzyme in solution acting on a solid starch substrate. Thus, the surface area accessible to enzyme and the efficiency of adsorption of enzyme onto this surface are critical kinetic parameters (Bertoft & Manelius, 1992). The sizes of lotus rhizome starch granules are larger than that of seed starch granules (Fig. 1). Larger rhizome starch granules have lower granule surface area to volume, so rhizome starches had a lower rate of enzyme hydrolysis than seed starches. It is also reported that the A-, B- and C-type starches show different susceptibilities to α-amylase hydrolysis. Generally, the B- or C-type starch shows more resistance to enzyme hydrolysis than A-type starch (Tester, Karkalas, & Qi, 2004). C-type starch from lotus rhizome also had a higher resistance to α-amylase hydrolysis than A-type starch from lotus seed. Therefore, compared with seed starches, larger granule size and C-type crystalline in lotus rhizome starches led to higher resistance to PPA.

The hydrolysis of lotus seed and rhizome starches by AGG was also biphasic, a relatively rapid hydrolysis of the amorphous region at the initial stage, followed by a progressively decreased rate thereafter (Fig. 5c). Glucoamylase is an exo-amylase that produces D-glucose from the nonreducing ends of starch chains. Susceptibility of starch to AAG attack is influenced by factors such as amylose to amylopectin ratio, crystalline structure, particle size and relative surface area, granule integrity, porosity of granules, and structural inhomogeneities (Blazek & Copeland, 2010). Though lotus seed and rhizome starches had different amylose contents, crystalline structure, and particle size, they showed similar hydrolysis rate by AGG. After 72 h, seed and rhizome starches were respectively hydrolyzed to the extent of 83.5% and 81.0%.

4. Conclusion

In conclusion, native starches were isolated from lotus seed and rhizome, and their physicochemical properties were investigated. Seed starch granules were oval in shape with a central hilum and a typical Maltese cross. Rhizome starches were mostly elongated in shape with a hilum and a Maltese cross at one end of granule, and some starch granules were oval in shape with a central hilum and a typical Maltese cross. The average particle size (the long axis length) was 9.73, 26.63, 17.86 and 34.42 μm for seed starch, rhizome total starch, rhizome oval starch and rhizome elongated starch, respectively. Seed starches showed higher amylose content and gelatinization temperature, and lower swelling power than rhizome starch. Seed starches exhibited an A-type crystalline and rhizome starches showed a C-type crystalline, a combination of A- and B-type allomorphs. The B-type allomorph existed in the interior of C-type rhizome starch granule, which was surrounded by the A-type allomorph at the periphery of starch granule. Rhizome starch had higher ordered structure at starch external region than seed starch. Rhizome starch crystalline changed from C- to A-type, and the degree of order at starch external region increased during acid hydrolysis. Seed starch had lower hydrolysis degree of acid, higher hydrolysis degree of PPA than rhizome starch. While AAG hydrolysis was similar between seed and rhizome starches. These results would be useful for various applications of lotus starches in food and nonfood industry.

Acknowledgments

This study was financially supported by grants from the National Natural Science Foundation of China (31071342 and 31170299) and the Priority Academic Program Development of Jiangsu Higher Education Institutions.

References

Bertoft, E., & Manelius, R. (1992). A method for the study of the enzymatic hydrolysis of starch granules. *Carbohydrate Research*, *227*, 269–283.
Bhat, R., & Sridhar, K. R. (2008). Nutritional quality evaluation of electron beam-irradiated lotus (*Nelumbo nucifera*) seeds. *Food Chemistry*, *107*, 174–184.
Blazek, J., & Copeland, L. (2010). Amylolysis of wheat starches. II. Degradation patterns of native starch granules with varying functional properties. *Journal of Cereal Science*, *52*, 295–302.
Bogracheva, T. Y., Morris, V. J., Ring, S. G., & Hedley, C. L. (1998). The granular structure of C-type pea starch and its role in gelatinization. *Biopolymers*, *45*, 323–332.
Cheetham, N. W. H., & Tao, L. (1998). Variation in crystalline type with amylose content in maize starch granules: An X-ray powder diffraction study. *Carbohydrate Polymers*, *36*, 277–284.
Harrigan, K. A. (1997). Particle size analysis using automated image analysis. *Cereal Foods World*, *42*, 30–35.
Hermansson, A. M., & Svegmark, K. (1996). Developments in the understanding of starch functionality. *Trends in Food Science and Technology*, *7*, 345–353.
Konik-Rose, C., Thistleton, J., Chanvrier, H., Tan, I., Halley, P., Gidley, M., et al. (2007). Effects of starch synthase IIa gene dosage on grain, protein and starch in endosperm of wheat. *Theoretical and Applied Genetics*, *115*, 1053–1065.
Lawal, O. S., Adebowale, K. O., Ogunsanwo, B. M., Barba, L. L., & Ilo, N. S. (2005). Oxidized and acid thinned starch derivatives of hybrid maize: Functional characteristics, wide-angle X-ray diffractometry and thermal properties. *International Journal of Biological Macromolecules*, *35*, 71–79.
Lee, H. K., Choi, Y. M., Noh, D. O., & Suh, H. J. (2005). Antioxidant effect of Korean traditional lotus liquor (Yunyupju). *International Journal of Food Science and Technology*, *40*, 709–715.
Li, J. H., Vasanthan, T., Hoover, R., & Rossnagel, B. G. (2004). Starch from hull-less barley: V. *In-vitro* susceptibility of waxy, normal, and high-amylose starches towards hydrolysis by alpha-amylases and amyloglucosidase. *Food Chemistry*, *84*, 621–632.
Li, J. H., Vasanthan, T., Rossnagel, B., & Hoover, R. (2001). Starch from hullless barley: II. Thermal, rheological and acid hydrolysis characteristics. *Food Chemistry*, *74*, 407–415.
Lii, C. Y., & Lee, B. L. (1993). Heating A-, B-, and C-type starches in aqueous sodium chloride: Effects of sodium chloride concentration and moisture content on differential scanning calorimetry thermograms. *Cereal Chemistry*, *70*, 188–192.
Lin, H. M., Chang, Y. H., Lin, J. H., Jane, J. L., Sheu, M. J., & Lu, T. J. (2006). Heterogeneity of lotus rhizome starch granules as revealed by α-amylase degradation. *Carbohydrate Polymers*, *66*, 528–536.
Lindeboom, N., Chang, P. R., & Tyler, R. T. (2004). Analytical, biochemical and physicochemical aspects of starch granule size, with emphasis on small granule starches: A review. *Starch*, *56*, 89–99.
Liu, C. P., Tsai, W. J., Lin, Y. L., Liao, J. F., Chen, C. F., & Kuo, Y. C. (2004). The extracts from *Nelumbo nucifera* suppress cell cycle progression, cytokine genes expression, and

cell proliferation in human peripheral blood mononuclear cells. *Life Sciences*, *75*, 699–716.
Pérez, S., Baldwin, P. M., & Gallant, D. J. (2009). Structural features of starch granules I. In J. BeMiller, & R. Whistler (Eds.), *Starch: Chemistry and technology* (3rd ed., pp. 149–192). Elsevier Academic Press.
Rai, S., Wahile, A., Mukherjee, K., Saha, B. P., & Mukherjee, P. K. (2006). Antioxidant activity of *Nelumbo nucifera* (sacred lotus) seeds. *Journal of Ethnopharmacology*, *104*, 322–327.
Sandhu, K. S., Singh, N., & Kaur, M. (2004). Characteristics of the different corn types and their grain fractions: Physicochemical, thermal, morphological, and rheological properties of starches. *Journal of Food Engineering*, *64*, 119–127.
Sevenou, O., Hill, S. E., Farhat, I. A., & Mitchell, J. R. (2002). Organisation of the external region of the starch granule as determined by infrared spectroscopy. *International Journal of Biological Macromolecules*, *31*, 79–85.
Shad, M. A., Nawaz, H., Hussain, M., & Yousuf, B. (2011). Proximate composition and functional properties of rhizomes of lotus (*Nelumbo nucifera*) from Punjab, Pakistan. *Pakistan Journal of Botany*, *43*, 895–904.
Srichuwong, S., Isono, N., Mishima, T., & Hisamatsu, M. (2005). Structure of lintnerized starch in related to X-ray diffraction pattern and susceptibility to acid and enzyme hydrolysis of starch granules. *International Journal of Biological Macromolecules*, *37*, 115–121.
Suzuki, A., Kaneyama, M., Shibanuma, K., Takeda, Y., Abe, J., & Hizukuri, S. (1992). Characterization of lotus starch. *Cereal Chemistry*, *69*, 309–315.
Tester, R. F., Karkalas, J., & Qi, X. (2004). Starch structure and digestibility enzyme–substrate relationship. *Worlds Poultry Science Journal*, *60*, 186–195.
Tester, R. F., & Morrison, W. R. (1990). Swelling and gelatinization of cereal starches. I. Effects of amylopectin, amylose and lipids. *Cereal Chemistry*, *67*, 551–557.
Wang, L. F., & Wang, Y. J. (2001). Structures and physicochemical properties of acid-thinned corn, potato and rice starches. *Starch*, *53*, 570–576.
Wang, S. J., Yu, J. L., Yu, J. G., Chen, H. X., & Pang, J. P. (2007). The effect of acid hydrolysis on morphological and crystalline properties of Rhizoma *Dioscorea* starch. *Food Hydrocolloids*, *21*, 1217–1222.
Wang, Q. C., & Zhang, X. Y. (2004). *Lotus flower cultivars in China*. Beijing: China Forestry Publishing House., 296 pp.
Wei, C. X., Qin, F. L., Zhou, W. D., Chen, Y. F., Xu, B., Wang, Y. P., et al. (2010). Formation of semi-compound C-type starch granule in high-amylose rice developed by antisense RNA inhibition of starch-branching enzyme. *Journal of Agricultural and Food Chemistry*, *58*, 11097–11104.
Wei, C. X., Qin, F. L., Zhou, W. D., Xu, B., Chen, C., Chen, Y. F., et al. (2011). Comparison of the crystalline properties and structural changes of starches from high-amylose transgenic rice and its wild type during heating. *Food Chemistry*, *128*, 645–652.
Wei, C. X., Qin, F. L., Zhu, L. J., Zhou, W. D., Chen, Y. F., Wang, Y. P., et al. (2010). Microstructure and ultrastructure of high-amylose rice resistant starch granules modified by antisense RNA inhibition of starch branching enzyme. *Journal of Agricultural and Food Chemistry*, *58*, 1224–1232.
Wei, C. X., Xu, B., Qin, F. L., Yu, H. G., Chen, C., Meng, X. L., et al. (2010). C-type starch from high-amylose rice resistant starch granules modified by antisense RNA inhibition of starch branching enzyme. *Journal of Agricultural and Food Chemistry*, *58*, 7383–7388.
Xu, S. Y., & Shoemaker, C. F. (1986). Gelatinization properties of Chinese water chestnut starch and lotus root starch. *Journal of Food Science*, *51*, 445–449.
Zhong, G., Chen, Z. D., & We, Y. M. (2007). physicochemical properties of lotus (*Nelumbo nucifera* Gaertn.) and kudzu (*Pueraria hirsute* Matsum.) starches. *International Journal of Food Science and Technology*, *42*, 1449–1455.
Zhou, Y., Hoover, R., & Liu, Q. (2004). Relationship between α-amylase degradation and the structure and physicochemical properties of legume starches. *Carbohydrate Polymers*, *57*, 299–317.